# Crystal Structure and Properties of $Ba_{11}FeTi_{27}O_{66.5}$

**Terrell A. Vanderah,*[a] Theo Siegrist,[b] Robert S. Roth,[a] Arthur P. Ramirez,[b] and Richard G. Geyer[c]**

**Keywords:** Mixed metal oxides / X-ray diffraction / Magnetic susceptibility / Dielectric constants / Dielectric loss tangent

The crystal structure of $Ba_{11}FeTi_{27}O_{66.5}$ was determined using single-crystal and powder X-ray diffraction methods. This phase crystallizes in the monoclinic space group *C*2/*m* (No. 12) (*a* = 23.324(1) Å, *b* = 11.388(1) Å, *c* = 9.8499(3) Å, β = 90.104(3)°; *Z* = 2; $\rho_{calcd.}$ = 4.98 g/cm$^3$), and exhibits a 10-layer structure built from close-packed [O,(Ba,O)] layers with a stacking sequence $(cchhc)_2$. Octahedral sites are occupied by a mixture of $Fe^{3+}$ and $Ti^{4+}$, with some preferential ordering suggested by analysis of bond valence sums. The structure features vertex-, edge-, and face-sharing of the [Ti(Fe)$O_6$] octahedra. Indexed X-ray powder diffraction data for a polycrystalline specimen are given. $Ba_{11}FeTi_{27}O_{66.5}$ and the 8-layer phase $Ba_4Fe_2Ti_{10}O_{27}$ are built from the same types of polyhedral layers, some of which feature vacant sites between two Ba ions, which substitute for three oxygens in a row. The single-crystal results suggest that the basic structural formula of the phase is $A_{11}B_{28}O_{66+x}$, with the value of x (and hence the Fe/Ti ratio) determined by partial occupancy of one of these vacant sites. Variation of this occupancy factor with synthesis temperature may account for apparent slight differences in the stoichiometry of this phase in polycrystalline and single-crystal form. However, solid solution formation was not observed for polycrystalline specimens. A comparison of the crystal structure obtained for $Ba_{11}FeTi_{27}O_{66.5}$ with that previously proposed for "$Zr^{4+}$-stabilized $Ba_2Ti_5O_{12}$" indicates that the phase "$Ba_2Ti_5O_{12}$" is actually a ternary compound which forms upon addition (either deliberately or inadvertently) of a trivalent ion such as $Fe^{3+}$ or $Al^{3+}$. The specimens $Ba_{11}Al_2Ti_{26}O_{66}$, $Ba_{11}Al_2Ti_{24}Sn_2O_{66}$, and $Ba_{11}Al_2Ti_{24}Zr_2O_{66}$ were also prepared and were found to form the $A_{11}B_{28}O_{66+x}$-type phase. $Ba_{11}FeTi_{27}O_{66.5}$ exhibits paramagnetic behavior that deviates somewhat from the Curie–Weiss Law below 75 K. Application of this formalism to the $1/\chi$ vs. *T* data above 75 K yields an effective moment consistent with the presence of high-spin $Fe^{3+}$ (*S* = 5/2), and a negative Weiss constant (about –25 K) indicating weak cooperative magnetic interactions that are overall antiferromagnetic. The relative permittivity and dielectric loss tangent of a sintered polycrystalline disk were measured at 5.33 GHz, yielding values (corrected for theoretical density) of 55 and 7.7(±0.3) × 10$^{-4}$, respectively.



## Introduction

Ceramic magnetic oxides serve important functions in a wide variety of electronic applications, including wireless communications. For example, circulators and isolators contain ceramic magnets that provide a static magnetic field to interact with the propagating microwave, thus steering and conditioning the signal. The properties required for such ceramics include large saturation magnetization, low dielectric loss, and a high dielectric constant. Materials currently in use include various garnets, spinels, and hexaferrites,[1,2] which exhibit relatively low relative permittivities (about 15). New materials with larger permittivities would permit miniaturization of these components. To this end, the $BaO:Fe_2O_3:TiO_2$ phase diagram has been systematically investigated[3] to elucidate compounds forming between the high-dielectric-constant polytitanates (e.g. $Ba_2Ti_9O_{19}$ and $BaTi_4O_9$), and strongly magnetic compounds such as barium hexaferrite ($BaFe_{12}O_{19}$). The phase diagram study confirmed the formation of a number of ternary phases with new structural types, including the title compound, denoted previously as phase "G"[3] with a stoichiometry close to "$Ba_{14}Fe_2Ti_{35}O_{87}$" (= 0.28:0.02:0.70 $BaO:Fe_2O_3:TiO_2$), as estimated by the disappearing phase method. The present report describes the crystal structure and more precise stoichiometry of this compound, as determined by single-crystal and X-ray powder diffraction methods, and characterization of its dielectric and magnetic properties. In addition, the relationship between this ternary phase and the compound reported as "$Ba_2Ti_5O_{12}$" is described.

[a] National Institute of Standards and Technology, Materials Science and Engineering Laboratory
Gaithersburg, MD 20899, USA
[b] Bell Laboratories, Lucent Technologies
600 Mountain Ave, Murray Hill, NJ 07974, USA
[c] National Institute of Standards and Technology, Electronics and Electrical Engineering Laboratory
Boulder, CO 80305, USA

## Results and Discussion

### Description of the Crystal Structure and Stoichiometry

The results of the single-crystal structure determination are given in Table 1. Selected bond lengths and bond-val-

ence sums are collected in Table 2, and indexed experimental X-ray powder diffraction data for a polycrystalline specimen are given in Table 3. As seen in Table 1, electron density was observed at the O22 site indicating a partial occupancy factor of 0.24(7), resulting in an overall stoichiometry of $Ba_{11}FeTi_{27}O_{66.5}$ ($BaO:Fe_2O_3:TiO_2$ = 0.2857:0.0130:0.7013) ($Z$ = 2). With site O22 empty, the overall stoichiometry would be $Ba_{11}Fe_2Ti_{26}O_{66}$ (= 0.2895:0.0263:0.6842 $BaO:Fe_2O_3:TiO_2$). The basic structural formula for this phase is therefore $A_{11}B_{28}O_{66+x}$, where A = $Ba^{2+}$ and B = $Ti^{4+}$, substituted with a small amount (<10 atom%) of a trivalent metal which determines the value of $x$. The subsolidus study[3] of the system at 1260 °C suggested little, if any, solid solution formation for this phase, and several closely spaced specimens indicated that the phase forms near the stoichiometry 0.28:0.02:0.70 $BaO:Fe_2O_3:TiO_2$, which is closer to the first formula with less Fe and a higher oxygen content. However, two polycrystalline specimens subsequently prepared precisely at $Ba_{11}FeTi_{27}O_{66.5}$ and $Ba_{11}Fe_2Ti_{26}O_{66}$ were not single-phase, despite repeatedly heating for hundreds of hours. The former composition contained small amounts (several %) of $BaTi_2O_5$ and $Ba_6Ti_{17}O_{40}$, while the latter contained an appreciable amount (>10%) of $Ba_4Fe_2Ti_{10}O_{27}$. According to the subsolidus phase diagram,[3] this suggests that at 1260° the compound forms with a composition between $Ba_{11}FeTi_{27}O_{66.5}$ and $Ba_{11}Fe_2Ti_{26}O_{66}$, with a lower O22 site occupancy factor than that determined for crystals grown by cooling from 1390 °C. As discussed below, these slight variations in Fe/Ti/O stoichiometry (note, however, that the A-cation/B-cation ratios remain constant) are readily accommodated by the crystal structure, and have been observed for other compounds occurring in the $BaO:Fe_2O_3:TiO_2$ system.[3–5] For convenience, the compound in the present study is referred to as $Ba_{11}FeTi_{27}O_{66.5}$, according to Table 1. The X-ray powder pattern, calculated using the single-crystal results (Table 1) and the refined unit cell (Table 3), is in excellent agreement with the pattern observed for a polycrystalline sample (0.28:0.02:0.70 $BaO:Fe_2O_3:TiO_2$) of this phase, as shown in Figure 1.

The structure of $Ba_{11}FeTi_{27}O_{66.5}$ may be described as a 10-layer (*10L*) close-packed (*cp*) arrangement built from [O] and [Ba,O] layers, stacked along the *a*-axis, with the transition metals occupying octahedral interstices. The connectivity of the structure includes vertex-, edge-, and face-sharing of [$(Ti^{4+}/Fe^{3+})O_6$] octahedra. The *a*-parameter of the unit cell indicates an average *cp* layer thickness of 2.362 Å, which is similar to that observed for other close-packed structures in this chemical system.[6,7] The arrangement is illustrated in Figure 2, as viewed along the ⟨011⟩ direction to reveal the stacking pattern of the cubic (*ccp*), and hexagonal (*hcp*) close-packed layers. The stacking sequence is $(cchhc)_2$ (*c* denotes a cubic close-packed layer and *h* denotes a hexagonally close-packed layer), where octahedral interstices share faces across *hcp* layers. In pairs of face-sharing octahedra that are occupied, the cations are displaced away from each other resulting in cation-cation distances of the order of 2.7 Å to 2.8 Å.

Table 1. Structural Parameters obtained for $Ba_{11}FeTi_{27}O_{66.5}$, M = $Ti^{4+}(Fe^{3+})$

| Atom | Site | x | *y* | *z* | $100*U_{iso}$ | occ. |
|---|---|---|---|---|---|---|
| Ba 1 | 2a | 0 | 0 | 0 | 1.58(12) | |
| Ba 2 | 4h | 1/2 | 0.22715(23) | 1/2 | 1.61(8) | |
| Ba 3 | 4i | 0.89468(9) | 0 | 0.67147(22) | 1.01(7) | |
| Ba 4 | 8j | 0.60238(7) | 0.22859(16) | 0.83942(16) | 1.51(6) | |
| Ba 5 | 4i | 0.78713(10) | 0 | 0.33795(24) | 1.46(8) | |
| M 1 | 8j | 0.34924(21) | 0.1378(5) | 0.7628(5) | 1.48(15) | |
| M 2 | 8j | 0.45461(18) | 0.2624(4) | 0.8370(4) | 1.03(13) | |
| M 3 | 4i | 0.0494(3) | 0 | 0.6582(7) | 0.94(20) | |
| M 4 | 4i | 0.3580(3) | 0 | 0.4872(7) | 1.36(23) | |
| M 5 | 8j | 0.74963(19) | 0.1340(5) | 0.7190(5) | 1.37(15) | |
| M 6 | 4i | 0.1401(3) | 0 | 0.9918(7) | 1.01(21) | |
| M 7 | 4i | 0.2617(3) | 0 | 0.0032(7) | 1.10(21) | |
| M 8 | 8j | 0.14852(20) | 0.7558(4) | 0.5063(5) | 1.13(15) | |
| M 9 | 4f | 1/4 | 3/4 | 0 | 1.50(24) | |
| M10 | 4i | 0.5373(3) | 0 | 0.1630(8) | 2.1(3) | |
| O1 | 4i | 0.6040(10) | 0 | 0.3246(23) | 0.66(6) | |
| O2 | 8j | 0.5024(7) | 0.1329(15) | 0.2383(16) | 0.66(6) | |
| O3 | 4g | 0 | 0.2386(21) | 0 | 0.66(6) | |
| O4 | 2c | 0 | 0 | 1/2 | 0.66(6) | |
| O5 | 4i | 0.8988(10) | 0 | 0.1725(23) | 0.66(6) | |
| O6 | 8j | −0.0025(7) | 0.1224(14) | 0.2513(16) | 0.66(6) | |
| O7 | 8j | 0.3988(7) | 0.1292(15) | 0.4214(16) | 0.66(6) | |
| O8 | 8j | 0.1013(7) | 0.2441(15) | 0.3195(16) | 0.66(6) | |
| O9 | 8j | 0.9019(7) | 0.1310(15) | 0.4211(16) | 0.66(6) | |
| O10 | 8j | 0.1986(7) | 0.1326(15) | 0.4192(16) | 0.66(6) | |
| O11 | 8j | 0.2100(7) | 0.2511(15) | 0.1709(16) | 0.66(6) | |
| O12 | 8j | 0.5962(7) | 0.1267(14) | 0.0957(16) | 0.66(6) | |
| O13 | 8j | 0.2979(7) | 0.1300(15) | 0.0900(16) | 0.66(6) | |
| O14 | 8j | 0.0970(7) | 0.1203(15) | 0.0786(16) | 0.66(6) | |
| O15 | 8j | 0.6889(7) | 0.1256(14) | 0.4118(16) | 0.66(6) | |
| O16 | 4i | 0.2937(10) | 0 | 0.3369(23) | 0.66(6) | |
| O17 | 4i | 0.6973(10) | 0 | 0.1673(23) | 0.66(6) | |
| O18 | 8j | 0.3044(7) | 0.2488(15) | 0.3389(16) | 0.66(6) | |
| O19 | 4i | 0.2099(10) | 0 | 0.1806(23) | 0.66(6) | |
| O20 | 8j | 0.7998(7) | 0.1130 (15) | 0.0609(16) | 0.66(6) | |
| O21 | 2b | 1/2 | 0 | 0 | 0.66(6) | |
| O22 | 4i | 0.401(4) | 0 | 0.210(10) | 0.66(6) | 0.24(7) |

The polyhedral arrangements within each of the ten layers in the $Ba_{11}FeTi_{27}O_{66.5}$ structure are shown in Figure 3. This compound and $Ba_4Fe_2Ti_{10}O_{27}$ [6] (isostructural with $Ba_4Al_2Ti_{10}O_{27}$ [8]) are built from the same three types of layers: the first type contains strings of three edge-sharing octahedra plus isolated octahedra (layers 1,5,6,10), the second contains groups of five edge-sharing octahedra plus isolated octahedra (layers 2,4,7,9), and a third type contains continuous zigzag strips of edge-sharing octahedra (layers 3,8). The *8L* phase $Ba_4Fe_2Ti_{10}O_{27}$ [6] is built from two layers of the first type, four layers of the second type, and two layers of the third type (Figure 3 of ref.[6]). Not surprisingly, these two phases occur in equilibrium with one another.[3] The similarity of the two structures suggests that intergrowths between them may form easily, and could be the source of the relatively high residual in the structure refinement.

An interesting crystal-chemical feature, reminiscent of the barium polytitanates,[9] is the occurrence of vacancies in the oxygen/barium *cp* layers. As seen in Figure 3, and shown in detail in Figure 4, the vacancies occur in the first

  

Table 2. Selected bond lengths and cation bond valence sums (BVS)* for $Ba_{11}FeTi_{27}O_{66.5}$; * calculated using the formalism and parameters ($B$ = 0.37; $r_0$ values 2.285, 1.815, 1.759 for $Ba^{2+}$, $Ti^{4+}$, $Fe^{3+}$, respectively) from ref.[23]

| | | | | | | | |
|---|---|---|---|---|---|---|---|
| Ba 1 | −O3 | 2.718 (24) Å | (2 ×) | M 3 | −O4 | 1.939 (16) Å | |
| | −O5 | 2.912 (23) Å | (2 ×) | | −O5 | 2.060 (24) Å | |
| | −O6 | 2.844 (16) Å | (4 ×) | | −O6 | 1.985 (17) Å | (2 ×) |
| | −O14 | 2.757 (16) Å | (4 ×) | | −O9 | 2.032 (17) Å | (2 ×) |
| | *BVS* | *3.00* | | | *BVS($Ti^{4+}$)* | *3.62* | |
| Ba 2 | −O2 | 2.795 (16) Å | (2 ×) | | BVS($Fe^{3+}$) | *3.11* | |
| | −O4 | 3.108 (16) Å | | M 4 | −O1 | 2.056 (24) Å | |
| | −O6 | 2.992 (16) Å | (2 ×) | | −O7 | 1.870 (17) Å | (2 ×) |
| | −O7 | 2.723 (16) Å | (2 ×) | | −O15 | 2.059 (17) Å | (2 ×) |
| | −O8 | 2.979 (16) Å | (2 ×) | | −O16 | 2.109 (24) Å | |
| | −O9 | 2.908 (16) Å | (2 ×) | | *BVS($Ti^{4+}$)* | *3.75* | |
| | *BVS* | *2.21* | | | *BVS($Fe^{3+}$)* | *3.33* | |
| Ba 3 | −O4 | 2.985 (16) Å | | M 5 | −O10 | 1.822 (17) Å | |
| | −O6 | 2.976 (16) Å | (2 ×) | | −O11 | 1.959 (17) Å | |
| | −O8 | 2.784 (16) Å | (2 ×) | | −O13 | 2.187 (17) Å | |
| | −O9 | 2.890 (16) Å | (2 ×) | | −O16 | 1.911 (16) Å | |
| | −O10 | 2.796 (16) Å | (2 ×) | | −O18 | 1.904 (17) Å | |
| | −O14 | 2.826 (16) Å | (2 ×) | | −O19 | 2.050 (17) Å | |
| | −O19 | 2.844 (23) Å | | | *BVS($Ti^{4+}$)* | *4.12* | |
| | *BVS* | *2.57* | | | *BVS($Fe^{3+}$)* | *3.54* | |
| Ba 4 | −O2 | 2.780 (16) Å | | M 6 | −O5 | 1.858 (24) Å | |
| | −O3 | 2.892 (16) Å | | | −O14 | 1.904 (17) Å | (2 ×) |
| | −O5 | 3.094 (16) Å | | | −O19 | 2.472 (24) Å | |
| | −O6 | 3.019 (16) Å | | | −O20 | 1.973 (17) Å | (2 ×) |
| | −O7 | 2.810 (16) Å | | | *BVS($Ti^{4+}$)* | *3.95* | |
| | −O9 | 3.027 (16) Å | | | *BVS($Fe^{3+}$)* | *3.40* | |
| | −O12 | 2.785 (16) Å | | | | | |
| | −O13 | 2.675 (16) Å | | | −O13 | 1.908 (17) Å | (2 ×) |
| | −O14 | 2.922 (16) Å | | | −O17 | 1.935 (24) Å | |
| | −O18 | 2.809 (16)Å | | | −O19 | 2.128 (24) Å | |
| | −O20 | 3.070 (16) Å | | | −O20 | 2.029 (17) Å | (2 ×) |
| | −O22 | 2.650 (16) Å | | | *BVS($Ti^{4+}$)* | *3.85* | |
| | *BVS* | *2.61* | | | *BVS($Fe^{3+}$)* | *3.31* | |
| Ba 5 | −O5 | 3.076 (22) Å | | M 8 | −O7 | 1.953 (17) Å | |
| | −O9 | 3.174 (16) Å | (2 ×) | | −O8 | 2.146 (17) Å | |
| | −O10 | 2.851 (16) Å | (2 ×) | | −O9 | 1.887 (17) Å | |
| | −O15 | 2.799 (16) Å | (2 ×) | | −O10 | 1.928 (17) Å | |
| | −O17 | 2.686 (16) Å | | | −O15 | 1.990 (17) Å | |
| | −O18 | 2.889 (16) Å | (2 ×) | | −O18 | 1.882 (17) Å | |
| | −O20 | 3.034 (16) Å | (2 ×) | | *BVS($Ti^{4+}$)* | *4.13* | |
| | *BVS* | *2.23* | | | *BVS($Fe^{3+}$)* | *3.55* | |
| | | | | M 9 | −O11 | 1.927 (16) Å | (2 ×) |
| M 1 | −O1 | 2.098 (16) Å | | | −O13 | 1.977 (17) Å | (2 ×) |
| | −O8 | 1.949 (16) Å | | | −O20 | 2.037 (17) Å | (2 ×) |
| | −O11 | 1.986 (16) Å | | | *BVS($Ti^{4+}$)* | *3.88* | |
| | −O12 | 1.893 (16) Å | | | *BVS($Fe^{3+}$)* | *3.34* | |
| | −O15 | 1.943 (16) Å | | | | | |
| | −O17 | 2.031 (16) Å | | M10 | −O1 | 2.226 (24) Å | |
| | *BVS($Ti^{4+}$)* | *3.88* | | | −O2 | 1.879 (17) Å | (2 ×) |
| | *BVS($Fe^{3+}$)* | *3.34* | | | −O12 | 2.100 (17) Å | (2 ×) |
| | | | | | −O21 | 1.827 (13) Å | |
| M 2 | −O2 | 1.923 (16) Å | | | *BVS($Ti^{4+}$)* | *3.94* | |
| | −O3 | 1.924 (16) Å | | | *BVS($Fe^{3+}$)* | *3.39* | |
| | −O6 | 1.932 (16) Å | | | | | |
| | −O8 | 2.021 (17) Å | | | | | |
| | −O12 | 2.058 (17) Å | | | | | |
| | −O14 | 1.982 (17) Å | | | | | |
| | *BVS($Ti^{4+}$)* | *3.94* | | | | | |
| | *BVS($Fe^{3+}$)* | *3.39* | | | | | |

  

Table 3. X-ray powder diffraction data for $Ba_{11}FeTi_{27}O_{66.5}$; *C2/m*; $a = 23.324(1)$ Å, $b = 11.388(1)$ Å, $c = 9.8499(3)$ Å, $\beta = 90.104(3)°$

| *h* | *k* | *l* | $2\theta_{obs}$ | $I_{obs}$ | $2\theta_{calcd.}$ | $\Delta 2\theta$ | $d_{obs.}$ |
|---|---|---|---|---|---|---|---|
| 1 | 1 | 0 | 8.633 | 4 | 8.634 | −0.001 | 10.23 |
| −1 | 1 | 1 | 12.460 | <1 | 12.458 | 0.002 | 7.098 |
| 0 | 2 | 0 | 15.569 | 1 | 15.550 | 0.019 | 5.686 |
| 2 | 2 | 0 | 17.332 | 6 | 17.317 | 0.015 | 5.112 |
| −4 | 0 | 1 | 17.637 | 2 | 17.647 | −0.010 | 5.024 |
| 2 | 2 | 1 | 19.548 | 17 | 19.541 | 0.007 | 4.537 |
| 4 | 2 | 0 | 21.800 | 1 | 21.798 | 0.002 | 4.0735 |
| 5 | 1 | 1 | 22.481 | <1 | 22.483 | −0.002 | 3.9516 |
| 3 | 1 | 2 | 22.751 | 4 | 22.753 | −0.002 | 3.9053 |
| 4 | 2 | 1 | 23.622 | 25 | 23.625 | −0.003 | 3.7632 |
| 6 | 0 | 1 | 24.603 | 9 | 24.615 | −0.012 | 3.6153 |
| 2 | 2 | 2 | 25.082 | 5 | 25.086 | −0.004 | 3.5474 |
| 1 | 3 | 1 | 25.414 | 3 | 25.416 | −0.002 | 3.5018 |
| 3 | 3 | 0 | 26.120 | 2 | 26.102 | 0.018 | 3.4087 |
| 5 | 1 | 2 | 27.460 | <1 | 27.476 | −0.016 | 3.2453 |
| 3 | 3 | 1 | 27.668 | 5 | 27.659 | 0.009 | 3.2214 |
| 7 | 1 | 0 | 27.867 | <1 | 27.875 | −0.008 | 3.1989 |
| 2 | 0 | 3 | 28.216 | 19 | 28.227 | −0.011 | 3.1601 |
| 1 | 1 | 3 | 28.537 | 27 | 28.534 | 0.003 | 3.1253 |
| 6 | 2 | 1 | 29.249 | 100 | 29.246 | 0.003 | 3.0508 |
| 8 | 0 | 0 | 30.640 | 13 | 30.639 | 0.001 | 2.9154 |
| 0 | 2 | 3 | 31.429 | 84 | 31.426 | 0.003 | 2.8440 |
| −5 | 3 | 1 | 31.688 | 25 | 31.682 | 0.006 | 2.8213 |
| 3 | 3 | 2 | 31.911 | 36 | 31.900 | 0.011 | 2.8021 |
| −2 | 2 | 3 | 32.369 | 10 | 32.360 | 0.009 | 2.7635 |
| −7 | 1 | 2 | 33.352 | 7 | 33.353 | −0.001 | 2.6842 |
| −2 | 4 | 1 | 33.623 | 2 | 33.626 | −0.003 | 2.6632 |
| 5 | 1 | 3 | 34.300 | 2 | 34.315 | −0.015 | 2.6122 |
| 8 | 2 | 0 | 34.526 | 1 | 34.534 | −0.008 | 2.5956 |
| −4 | 2 | 3 | 35.051 | 1 | 35.051 | 0.000 | 2.5579 |
| −5 | 3 | 2 | 35.477 | 9 | 35.474 | 0.003 | 2.5282 |
| 8 | 2 | 1 | 35.753 | 20 | 35.766 | −0.013 | 2.5093 |
| −4 | 4 | 1 | 36.244 | 6 | 36.241 | 0.003 | 2.4764 |
| −1 | 3 | 3 | 36.347 | 6 | 36.347 | 0.000 | 2.4696 |
| −7 | 3 | 1 | 36.997 | 3 | 36.998 | −0.001 | 2.4277 |
| −2 | 0 | 4 | 37.273 | 7 | 37.276 | −0.003 | 2.4104 |
| −3 | 3 | 3 | 37.996 | 2 | 37.992 | 0.004 | 2.3662 |
| 10 | 0 | 0 | 38.570 | 12 | 38.568 | 0.002 | 2.3323 |
| 3 | 1 | 4 | 39.167 | 8 | 39.168 | −0.001 | 2.2981 |
| 4 | 4 | 2 | 39.686 | 49 | 39.681 | 0.005 | 2.2692 |
| −9 | 1 | 2 | 40.036 | 3 | 40.042 | −0.006 | 2.2502 |
| 6 | 4 | 1 | 40.293 | 8 | 40.295 | −0.002 | 2.2364 |
| −2 | 2 | 4 | 40.618 | <1 | 40.613 | 0.005 | 2.2193 |
| −5 | 3 | 3 | 41.130 | 2 | 41.122 | 0.008 | 2.1928 |
| 3 | 5 | 0 | 41.252 | 1 | 41.270 | −0.018 | 2.1866 |
| 9 | 3 | 0 | 42.191 | 9 | 42.187 | 0.004 | 2.1401 |
| −3 | 5 | 1 | 42.308 | 13 | 42.317 | −0.009 | 2.1344 |
| 2 | 4 | 3 | 42.737 | 8 | 42.720 | 0.017 | 2.1140 |
| −10 | 2 | 1 | 42.840 | 7 | 42.843 | −0.003 | 2.1091 |
| 4 | 2 | 4 | 42.925 | 6 | 42.904 | 0.021 | 2.1052 |
| 6 | 4 | −2 | 43.426 | 87 | 43.418 | 0.008 | 2.0820 |
| −1 | 5 | 2 | 43.926 | <1 | 43.932 | −0.006 | 2.0595 |
| −8 | 2 | 3 | 44.432 | 6 | 44.425 | 0.007 | 2.0372 |
| 8 | 2 | 3 | 44.519 | 4 | 44.499 | 0.020 | 2.0334 |
| 4 | 4 | 3 | 44.892 | 1 | 44.896 | −0.004 | 2.0174 |
| 5 | 5 | 1 | 45.227 | 11 | 45.221 | 0.006 | 2.0032 |
| −3 | 3 | 4 | 45.378 | 14 | 45.369 | 0.009 | 1.9969 |
| −6 | 2 | 4 | 46.387 | 2 | 46.400 | −0.013 | 1.9558 |
| 7 | 1 | 4 | 46.525 | 3 | 46.548 | −0.023 | 1.9503 |
| 12 | 0 | 0 | 46.692 | 1 | 46.694 | −0.002 | 1.9437 |
| −11 | 1 | 2 | 47.295 | <1 | 47.281 | 0.014 | 1.9203 |
| 8 | 4 | −2 | 48.296 | 47 | 48.290 | 0.006 | 1.8828 |
| 8 | 0 | 4 | 48.395 | 41 | 48.387 | 0.008 | 1.8792 |
| −1 | 5 | 3 | 48.775 | 15 | 48.774 | 0.001 | 1.8655 |
| 7 | 5 | 1 | 49.302 | 9 | 49.308 | −0.006 | 1.8468 |
| 2 | 6 | 1 | 49.490 | 11 | 49.490 | 0.000 | 1.8402 |
| 11 | 3 | 1 | 50.121 | 1 | 50.113 | 0.008 | 1.8185 |
| 12 | 2 | 1 | 50.437 | 24 | 50.444 | −0.007 | 1.8078 |
| −10 | 2 | 3 | 50.526 | 22 | 50.524 | 0.002 | 1.8048 |
| −5 | 1 | 5 | 50.892 | 3 | 50.876 | 0.016 | 1.7927 |
| 4 | 2 | 5 | 51.510 | 4 | 51.513 | −0.003 | 1.7727 |
| 7 | 3 | 4 | 52.082 | 6 | 52.082 | 0.000 | 1.7545 |
| 2 | 6 | 2 | 52.224 | 4 | 52.204 | 0.020 | 1.7501 |
| −13 | 1 | 1 | 52.394 | 6 | 52.394 | 0.000 | 1.7448 |
| 11 | 3 | 2 | 52.811 | 2 | 52.816 | −0.005 | 1.7320 |
| 4 | 6 | 2 | 54.082 | 18 | 54.084 | −0.002 | 1.6943 |
| −6 | 2 | 5 | 54.580 | 35 | 54.574 | 0.006 | 1.6800 |
| 1 | 5 | 4 | 55.032 | 1 | 55.021 | 0.011 | 1.6672 |
| 14 | 0 | 1 | 55.947 | 19 | 55.946 | 0.001 | 1.6421 |
| 2 | 6 | 3 | 56.530 | 2 | 56.519 | 0.011 | 1.6266 |
| 1 | 7 | 0 | 56.683 | 3 | 56.671 | 0.012 | 1.6225 |
| −9 | 5 | 2 | 56.890 | 3 | 56.910 | −0.020 | 1.6171 |
| 9 | 3 | 4 | 57.011 | 3 | 57.004 | 0.007 | 1.6140 |
| 12 | 4 | 0 | 57.342 | 1 | 57.352 | −0.010 | 1.6054 |
| −1 | 7 | 1 | 57.505 | 1 | 57.505 | 0.000 | 1.6013 |
| 3 | 1 | 6 | 57.954 | 1 | 57.957 | −0.003 | 1.5899 |
| −14 | 2 | 1 | 58.408 | 11 | 58.406 | 0.002 | 1.5787 |
| −5 | 5 | 4 | 58.580 | 9 | 58.575 | 0.005 | 1.5744 |
| −8 | 6 | 1 | 58.735 | 8 | 58.742 | −0.007 | 1.5706 |
| −13 | 1 | 3 | 59.132 | 3 | 59.145 | −0.013 | 1.5610 |
| −7 | 3 | 5 | 59.620 | 1 | 59.626 | −0.006 | 1.5494 |
| −13 | 3 | 2 | 59.961 | 1 | 59.962 | −0.001 | 1.5414 |
| −12 | 4 | 2 | 60.597 | 24 | 60.593 | 0.004 | 1.5268 |
| −4 | 2 | 6 | 60.758 | 18 | 60.750 | 0.008 | 1.5231 |
| −5 | 7 | 1 | 60.992 | 12 | 60.991 | 0.001 | 1.5178 |
| −3 | 7 | 2 | 61.106 | 12 | 61.107 | −0.001 | 1.5153 |
| 6 | 0 | 6 | 61.262 | 4 | 61.284 | −0.022 | 1.5118 |
| −1 | 3 | 6 | 61.612 | 2 | 61.624 | −0.012 | 1.5040 |
| −7 | 5 | 4 | 62.001 | 2 | 62.019 | −0.018 | 1.4955 |
| −11 | 3 | 4 | 62.688 | 1 | 62.688 | 0.000 | 1.4808 |
| −15 | 1 | 2 | 63.139 | <1 | 63.148 | −0.009 | 1.4713 |
| −5 | 7 | 2 | 63.361 | 2 | 63.362 | −0.001 | 1.4666 |
| 3 | 5 | 5 | 63.535 | 3 | 63.542 | −0.007 | 1.4631 |
| 7 | 1 | 6 | 63.717 | 1 | 63.714 | 0.003 | 1.4593 |
| 4 | 6 | 4 | 63.915 | 1 | 63.917 | −0.002 | 1.4553 |
| 7 | 7 | 1 | 64.391 | <1 | 64.382 | 0.009 | 1.4457 |
| 13 | 1 | 4 | 64.806 | 1 | 64.815 | −0.009 | 1.4374 |
| −8 | 6 | 3 | 65.072 | 2 | 65.080 | −0.008 | 1.4322 |
| 8 | 0 | 6 | 65.234 | 6 | 65.218 | 0.016 | 1.4290 |
| 0 | 4 | 6 | 65.570 | 48 | 65.590 | −0.020 | 1.4225 |
| 8 | 4 | 5 | 65.937 | 6 | 65.955 | −0.018 | 1.4155 |
| 11 | 5 | 3 | 66.647 | 6 | 66.634 | 0.013 | 1.4021 |
| 2 | 8 | 1 | 66.838 | 9 | 66.836 | 0.002 | 1.3985 |
| −15 | 1 | 3 | 66.986 | 6 | 66.994 | −0.008 | 1.3958 |
| −8 | 2 | 6 | 67.420 | <1 | 67.395 | 0.025 | 1.3879 |
| 15 | 3 | 2 | 67.848 | 17 | 67.829 | 0.019 | 1.3802 |
| 9 | 7 | 0 | 67.966 | 14 | 67.980 | −0.014 | 1.3780 |
| −3 | 1 | 7 | 68.145 | 5 | 68.144 | 0.001 | 1.3749 |
| −4 | 8 | 1 | 68.428 | 1 | 68.450 | −0.022 | 1.3699 |
| −7 | 5 | 5 | 68.923 | 5 | 68.947 | −0.024 | 1.3612 |
| −2 | 6 | 5 | 69.140 | 5 | 69.129 | 0.011 | 1.3575 |
| 13 | 3 | 4 | 69.386 | 1 | 69.370 | 0.016 | 1.3533 |
| −12 | 4 | 4 | 69.818 | 8 | 69.837 | −0.019 | 1.3460 |
| 12 | 2 | 5 | 69.972 | 11 | 69.978 | −0.006 | 1.3434 |

Table 3. *(Continued)*

  

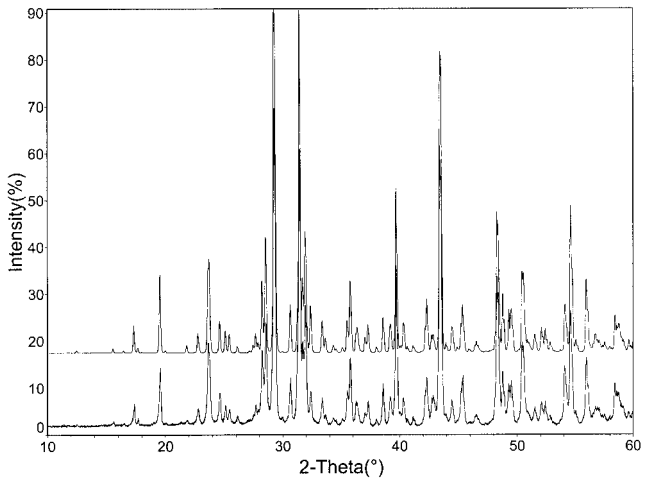


Figure 1. The X-ray powder diffraction pattern for $Ba_{11}FeTi_{27}O_{66.5}$ calculated from the single-crystal results (*top*) is in excellent agreement with the observed pattern (*bottom*) for a polycrystalline sample ($BaO:Fe_2O_3:TiO_2$ = 0.28:0.02:0.70); the stoichiometry of this phase in polycrystalline form (prepared at 1260°) apparently differs slightly from that of the single crystals (grown by cooling from 1390°), suggesting slightly different occupancy factors for the oxygen site O22 (Table 2); charge-balance is maintained by a corresponding change in the Fe/Ti ratio; in both cases, however, the A-cation/B-cation ratio remains the same (11:28)

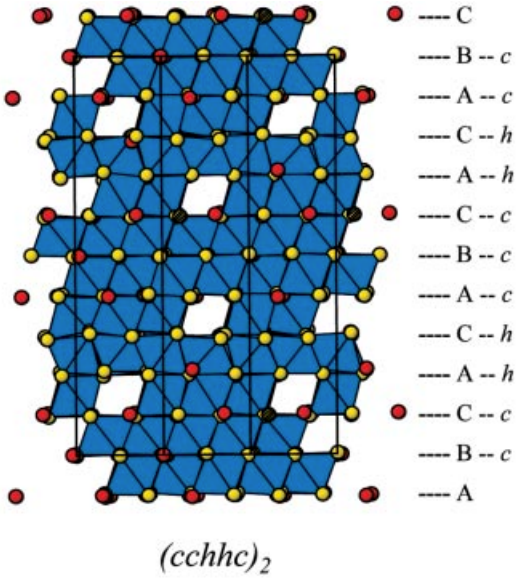


Figure 2. The crystal structure of *10L* $Ba_{11}FeTi_{27}O_{66.5}$ (*C2/m*; *a* = 23.324(1), *b* = 11.388(1), *c* = 9.8499(3) Å; β = 90.104(3)°] viewed approximately parallel to the close-packed (*cp*) [O,(Ba,O)] layers; the 10-layer stacking sequence is $(cchhc)_2$; the octahedra are occupied by $Ti^{4+}/Fe^{3+}$, with some preferential ordering suggested by analysis of bond valence sums; red spheres represent $Ba^{2+}$, yellow spheres represent oxygen with the hatched yellow spheres indicating the partially occupied O22 site (Table 2)

and second types of layers, where two Ba ions replace three oxygens in a row, reducing their coordination number from twelve to eleven. For $Ba_{11}FeTi_{27}O_{66.5}$, this results in a coordination number of 11 and a relatively low bond-valence sum for Ba2 (Table 2, Figure 4). The partially occupied site

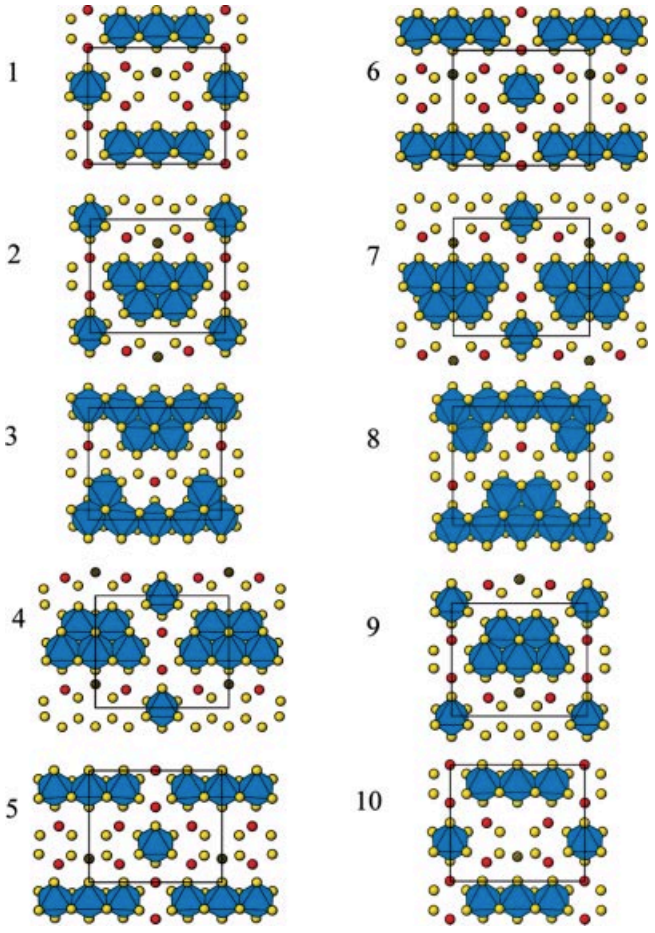


Figure 3. The structural arrangements within each of the ten layers of the close-packed structure of $Ba_{11}FeTi_{27}O_{66.5}$, viewed perpendicular to the layers; the representations are the same as in Figure 1; as seen here, the structure is built from three types of layers (*type 1* = layers 1,5,6,10; *type 2* = layers 2,4,7,9; *type 3* = layers 3,8); the same types of layers occur in the *8L* structure of $Ba_4Fe_2Ti_{10}O_{27}$; as observed for the barium polytitanate phases, the *cp* layers (types 1 and 2) are characterized by the occurrence of vacancies, wherein two Ba ions substitute for three oxygen positions in a row; the partially occupied O22 site (hatched yellow spheres) corresponds to one of these vacancies between two Ba ions

O22 corresponds to one of these *cp* vacancies, and occurs within bonding distance of Ba4 (Table 2, Figure 4). The occupancy factor of 0.24(7) for O22 obtained in the single-crystal study therefore suggests that 25% of the Ba4 sites are 12-coordinated and 75% are 11-coordinated.

The bond-valence sums about the M sites (Table 2) were calculated separately using the $r_0$ parameters for $Ti^{4+}$ and $Fe^{3+}$, and are generally consistent with the high Ti-content of this phase. However, site M3 was observed to have slightly longer bond lengths than the other sites, and returns a bond-valence sum suggesting preferential occupation by the slightly larger trivalent Fe ion (Table 3). The M3 sites occur in pairs of vertex-linked octahedra in adjacent layers of the first type described above (Figure 3, layers 1,5,6,107). Interestingly, the coordination sphere about M3 has no next-nearest neighbors within 3.5 Å, whereas the other M sites have from 3 to 9, with an average of 7, next-

  

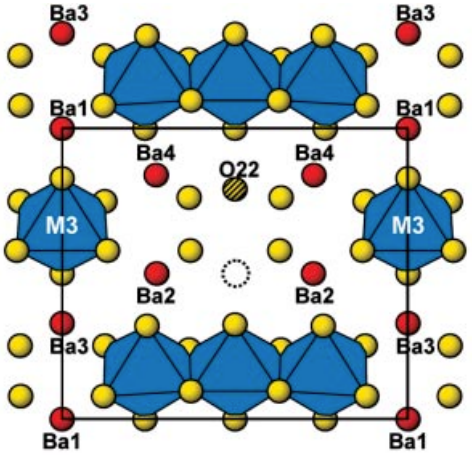


Figure 4. Magnified view of layer 1 in the structure of $Ba_{11}FeTi_{27}O_{66.5}$ (representations as in Figure 1), labeled to clarify the positions of the vacancies in the *cp* layers (dotted circle and hatched yellow O22 site); using the ligands on the upper and lower faces of the octahedra as a guide, the Ba2 sites are seen to occur in the lower *cp* layer, with the vacancy (dotted sphere) between them, thereby reducing their coordination number to eleven (Table 3); similarly, the Ba4 sites are seen to occur in the upper *cp* layer, but in this case the vacant site between them appears to be partially occupied (O22, Table 2), according to the electron density observed in the single-crystal study; note the marked displacement of O22 out of the *cp* row towards the interior of the unit cell; sites M3 occur in vertex-linked pairs of octahedra in adjacent layers, and exhibit bond-valence sums suggestive of preferential occupation by the somewhat larger $Fe^{3+}$ ion

nearest neighbors within this distance. The M3 sites are therefore unusually isolated in the structure, which may facilitate accommodation of a larger cation.

### Relationship to "$Ba_2Ti_5O_{12}$" (A Ternary Compound)

The synthesis, stability, and crystal chemistry of the phase referred to as "$Ba_2Ti_5O_{12}$" has long been of interest to researchers concerned with the phases occurring between $BaTiO_3$ and $TiO_2$, the so-called "barium polytitanates", which have technically important dielectric properties. The existence of $Ba_2Ti_5O_{12}$ was first reported by Jonker and Kwestroo[10] during the course of phase equilibria studies of the ternary systems with either $ZrO_2$ or $SnO_2$. They reported considerable solid solution of both oxides in the phase labeled $Ba_2Ti_5O_{12}$. However, many studies of the pure $BaO$-$TiO_2$ system failed to confirm the formation of this binary phase.[11–14] A subsequent study[15] found that "$Ba_2Ti_5O_{12}$" did not form in the ternary system with $SnO_2$, in contrast to the earlier report.[10] The phase did form, however, upon addition of $ZrO_2$. Small single crystals were grown and found to adopt a pseudo-orthorhombic unit cell with $a = 9.941$, $b = 11.482$, and $c = 23.528$ Å.[15] A later preliminary structural refinement of these crystals[16] suggested that the actual composition was $Ba_{11}(Ti,Zr)_{28}O_{66}O$, with the 67th oxygen in a position not located.[9] Subsequent chemical analyses of these crystals using an ion-microprobe[12] found about 0.25 wt% $Al_2O_3$ in addition to the expected amounts of BaO, $TiO_2$, and $ZrO_2$, although no alumina had been intentionally added. A comparison of the pseudo-orthorhombic unit cell for these crystals as well as the proposed crystal structure (Figure 10 in ref.[9]) reveals that they are essentially identical to those for $Ba_{11}FeTi_{27}O_{66.5}$ reported here (Table 1, Figure 3). Apparently, the phase "$Ba_2Ti_5O_{12}$" is actually a ternary compound stabilized by a relatively small content of a trivalent metal such as $Fe^{3+}$ or $Al^{3+}$. Note that the A:B:O A-cation:B-cation:oxygen ratios are very similar for all of these compositions. As previously noted,[10] Jonker and Kwestroo[4] "wet-milled" their specimens twice, once before and once after calcination, and this process is notorious for the introduction of impurities from the ceramic spheres used for milling. To confirm this, specimens with compositions $Ba_{11}Al_2Ti_{26}O_{66}$, $Ba_{11}Al_2Ti_{24}Sn_2O_{66}$, and $Ba_{11}Al_2Ti_{24}Zr_2O_{66}$ were synthesized (1250 °C, 1275 °C, and 1275 °C, respectively), and were all found to contain the $A_{11}B_{28}O_{66+x}$-type phase as the major product (>95%) [the phase was not observed to form in compositions with $Mg^{2+}$ or $Zn^{2+}$ (i.e. $Ba_{11}MgTi_{27}O_{66}$ or $Ba_{11}ZnTi_{27}O_{66}$)].

### Magnetic and Dielectric Properties of $Ba_{11}FeTi_{27}O_{66.5}$

The inverse magnetic susceptibility vs. temperature measured for $Ba_{11}FeTi_{27}O_{66.5}$ is shown in Figure 5. The behavior is paramagnetic, with highly dilute magnetic species, and follows the Curie–Weiss law above about 75 K. The slight curvature below 75 K and the extrapolated temperature intercept of −25 K indicate weak cooperative interactions between Fe spins that are, overall, antiferromagnetic in nature. Application of the Curie–Weiss formalism to the near-linear data above 75 K yields an effective moment of 5.2 $\mu_\beta$/Fe, which is similar to the free-ion spin-only moment for high-spin $Fe^{3+}$ ($S = 5/2$; 5.9 $\mu_\beta$/Fe).

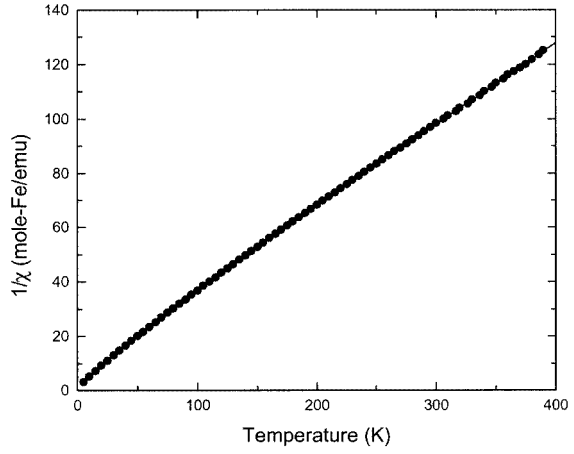


Figure 5. Inverse magnetic susceptibility vs. temperature for $Ba_{11}FeTi_{27}O_{66.5}$; the slight curvature below 75 K and the extrapolated temperature intercept of −25 K indicate weak cooperative interactions among the magnetic species that are overall antiferromagnetic in nature; the effective magnetic moment calculated from the essentially linear data above 75 K is consistent with the presence of high-spin $Fe^{3+}$

  

A corrected relative permittivity of 55, and a dielectric loss tangent, tanδ, of 7.7(±0.3) × $10^{-4}$ were obtained for $Ba_{11}FeTi_{27}O_{66.5}$. Both values were essentially independent of frequency between 5.0 and 5.5 GHz. Using Shannon's values for atomic polarizabilities and the Clausius−Mosotti theory,[18] a dielectric constant of 45 was estimated for this compound, a value in fair agreement with the experimental results given the uncertainty of the porosity measurement.

## Conclusions

The crystal structure of the new ternary oxide $Ba_{11}FeTi_{27}O_{66.5}$ has been characterized by single-crystal and powder X-ray diffraction methods. The compound adopts a monoclinic *10L* structure built from close-packed (*cp*) [O,(Ba,O)] layers with a stacking sequence $(cchhc)_2$. Octahedral sites are occupied by $Fe^{3+}$ and $Ti^{4+}$. The structure features vertex-, edge-, and face-sharing of the [Ti(Fe)$O_6$] octahedra. $Ba_{11}FeTi_{27}O_{66.5}$ is built from the same three types of layers as the neighboring *8L* compound $Ba_4Fe_2Ti_{10}O_{27}$. As observed for the binary barium polytitanates, some of the *cp* layers also feature vacant sites between two Ba ions which substitute for three oxygens in a row. The single-crystal structural results for $Ba_{11}FeTi_{27}O_{66.5}$ indicate that one of these sites is partially occupied, and that the basic structural formula for this phase is $A_{11}B_{28}O_{66+x}$, where A = $Ba^{2+}$ and B = $Ti^{4+}$ substituted with a small amount (<10 atom%) of a trivalent metal, which determines the value of $x$. The stoichiometry, or $x$-value, of the phase prepared in polycrystalline form at 1260 °C is slightly different from that of the crystals grown by cooling from 1390 °C, and occurs between the compositions $Ba_{11}FeTi_{27}O_{66.5}$ and $Ba_{11}Fe_2Ti_{26}O_{66}$. This variation in oxygen content and Fe/Ti ratio suggests that the partial occupancy site factor depends on the synthesis temperature. Interestingly, the phase apparently forms as a point compound in the subsolidus, with little or no solid solution formation. Analysis of the structural details using the bond valence method revealed one unusual B site, which was relatively expanded and isolated within the structure. This site is probably preferentially occupied by the larger, lower-valent $Fe^{3+}$ cations. The crystal structure obtained here for $Ba_{11}FeTi_{27}O_{66.5}$ is essentially identical to that proposed earlier for "$Zr^{4+}$-stabilized $Ba_2Ti_5O_{12}$"[9,15] crystals. The phase originally reported as "$Ba_2Ti_5O_{12}$"[10] is actually a ternary compound, which forms upon addition (either deliberately or inadvertently via, e.g., ball-milling) of a trivalent ion such as $Fe^{3+}$ or $Al^{3+}$. The specimens $Ba_{11}Al_2Ti_{26}O_{66}$ $Ba_{11}Al_2Ti_{24}Sn_2O_{66}$, and $Ba_{11}Al_2Ti_{24}Zr_2O_{66}$ were also prepared, and were found to form the $A_{11}B_{28}O_{66+x}$-type phase.

$Ba_{11}FeTi_{27}O_{66.5}$ was found to exhibit paramagnetic behavior above about 75 K. Application of the Curie−Weiss formalism to the $1/\chi$ vs. $T$ data above 75 K yielded an effective moment consistent with the presence of high-spin $Fe^{3+}$, and a negative Weiss constant (about −25 K) indicating weak cooperative magnetic interactions that are overall antiferromagnetic. The relative permittivity and dielectric loss tangent of a sintered polycrystalline disk were measured at 5.33 GHz, yielding values (corrected for theoretical density) of 55 and 7.7(±0.3) × $10^{-4}$, respectively.

## Experimental Section

Dark reddish-brown polycrystalline $Ba_{11}FeTi_{27}O_{66.5}$ was prepared by solid-state reaction of reagent-grade $BaCO_3$, $Fe_2O_3$, and phosphate-free $TiO_2$ in air in the molar ratio $BaO:Fe_2O_3:TiO_2$ = 0.28:0.02:0.70. Prior to each heating, the sample was ground for 15−20 min with an agate pestle and mortar, pressed into pellets, and placed on sacrificial powder of the same composition in an alumina combustion boat. After an initial overnight calcine at 1000 °C, four one-week heatings at 1260 °C resulted in a well crystallized, nearly single-phase* sample (10-g scale) [* the pattern contains two weak peaks ($I_{rel}$ < 0.8%), which can be attributed to $Ba_6Ti_{17}O_{40}$. Detection of small amounts of the phase $Ba_4Fe_2Ti_{10}O_{27}$ was precluded by peak overlap with the title phase]. Dark red platelet-like single crystals were obtained by slowly cooling (1 °C/h) a slightly non-stoichiometric liquid ($BaO:Fe_2O_3:TiO_2$ = 0.28:0.02:0.70) from 1390 °C to 1260 °C, followed by step-cooling to 800 °C, and then air-quenching. Samples were contained in platinum capsules (2.6 mm i.d.) open to the air. Crystals were harvested from dark prismatic chunks obtained by breaking the crystallized reaction mass, and were then characterized by the precession camera method (Zr-filtered Mo-$K_\alpha$ radiation) to assess quality, approximate cell parameters, and space group.

Single-crystal X-ray diffraction data were obtained with an Enraf−Nonius CAD-4 diffractometer (certain commercial equipment is identified in order to adequately specify the experimental procedure; recommendation or endorsement by the National Institute of Standards and Technology is not therein implied) using graphite-monochromated Mo-$K_\alpha$ radiation. A Gaussian integration absorption correction was applied to all measured intensities. Calculations were carried out using the NRCVAX[19] suite of programs. The structure was solved using Patterson and Fourier methods. Octahedral sites were assumed to be randomly occupied by $Ti^{4+}$ and a small amount (< 10 atom%) of $Fe^{3+}$. Since the contrast between Fe and Ti by X-ray diffraction is small, no attempt was made to directly refine their relative occupancies, and the scattering factor for Ti was used for atoms occupying the octahedral sites. The overall stoichiometry of the phase reported here was then deduced by simultaneous consideration of the following: 1) the disappearing phase method,[3] 2) charge balance in the presence of trivalent iron and tetravalent titanium, and 3) the degree of site occupancy of oxygen as indicated by the single-crystal X-ray diffraction data.

X-ray powder diffraction data were collected using a Philips diffractometer equipped with incident soller slits, theta-compensating slits, a 0.2 mm receiving slit, a graphite monochromator, and a scintillation detector. Data were collected at ambient temperature using Cu-$K_\alpha$ radiation with a 0.01° 2θ step size, and a 2 s count time. The sample was mounted in a welled glass slide. Intensity data, measured as relative peak heights above the background of hand-picked peaks, were obtained using the Jade 6 program suite. The observed 2θ line positions reported here were corrected using SRM 660, $LaB_6$,[20] as an external calibrating agent. The unit cell was refined from the corrected powder diffraction data (2θ values; Cu-$K_{\alpha 1}$ = 1.540593 Å) using the least-squares program CELLSVD.[21] During the refinement, the indices of selected peaks were fixed in

  

accordance with the powder pattern calculated using the results of the single-crystal X-ray study and the Jade program jPOWD.

The conditions used for the single-crystal structure determination are given in Table 4. Further details of the crystal-structure investigation may be obtained from the Fachinformationszentrum Karlsruhe, 76344 Eggenstein-Leopoldshafen, Germany, on quoting depository number CSD-413889.

Table 4. Experimental details for the single-crystal X-ray diffraction study of $Ba_{11}FeTi_{27}O_{66.5}$

| | |
|---|---|
| Crystal system | Monoclinic |
| Space group | *C 2/m* |
| Cell parameters | $a$ = 23.321(2) Å<br>$b$ = 11.384(1) Å<br>$c$= 9.847(1) Å<br>β = 90.09(1) °<br>$V$ = 2614.2(8) Å$^3$ |
| $Z$ | 2 |
| $\rho_{calcd.}$ [g cm$^{-3}$] | 4.98 |
| Crystal dimensions [mm] | 0.1 × 0.1 × 0.03 |
| μ [mm$^{-1}$] | 12.22 |
| 2θ (max) | 60° |
| Scan mode | T-scan |
| Reflections measured | 15759 |
| Unique reflections | 3954 |
| Reflections observed | 1656 |
| Transmission factors | 0.15−0.31 |
| Number of parameters | 157 |
| $R_F$ | 0.088 |
| $wR_F$ | 0.065 |

Magnetization was measured using a Quantum Design SQUID (Superconducting Quantum Interference Device) magnetometer. Measurements were made on a polycrystalline sample in a field of 0.5 Tesla between 400 K and 5 K. Magnetization measurements were carried out in fields up to 4 Tesla.

Permittivity and dielectric loss tangent measurements were performed at 5.33 GHz under ambient conditions using a sintered polycrystalline disk, approximately 11 mm in diameter and 87% dense. As described previously,[6,7] a dielectric resonator technique utilizing higher-order $TE_{0\gamma\nu}$ modes was used that allows the measurement of dielectric properties of a single sample at several contiguous frequency sub-bands. Corrections to the crystallographic density were incorporated by estimating the pore volume of the sample (from size and mass), and applying the Bruggeman effective medium formulation[22] for a two-phase composite. Uncertainties in the measurement of pore volume suggest a realistic accuracy limit for the permittivity values of ±10%, confirmed by measurements of similarly dense test samples such as $LaAlO_3$,[6] for which reliable single-crystal data are available.


[1] G. Geiger, *Bull. Am. Ceram. Soc.* **1994**, *73*, 57−61.
[2] T. Abraham, *Bull. Am. Ceram. Soc.* **1994**, *73*, 62−65.
[3] T. A. Vanderah, J. M. Loezos, R. S. Roth, *J. Solid State Chem.* **1996**, *121*, 38−50.
[4] I. E. Grey, C. Li, L. M. D. Cranswick, R. S. Roth, T. A. Vanderah, *J. Solid State Chem.* **1998**, *135*, 312−321.
[5] T. A. Vanderah, W. Wong-Ng, B. H. Toby, V. M. Browning, R. G. Geyer, R. D. Shull, R. S. Roth, *J. Solid State Chem.* **1999**, *143*, 182−197.
[6] T. A. Vanderah, W. Wong-Ng, Q. Huang, R. S. Roth, R. G. Geyer, R. B. Goldfarb, *J. Phys. Chem. Solids* **1997**, *58*, 1403−1415.
[7] T. Siegrist, T. A. Vanderah, A. P. Ramirez, R. G. Geyer, R. S. Roth, *J. Alloys and Comp.* **1998**, *274*, 169−178.
[8] J. Schmachtel, H. Mueller-Buschbaum, *Z. Anorg. Allg. Chem.* **1981**, *472*, 89−94.
[9] R. S. Roth, C. J. Rawn, C. G. Lindsay, W. Wong-Ng, *J. Solid State Chem.* **1993**, *104*, 99−118.
[10] G. H. Jonker, W. Kwestroo, *J. Am. Ceram. Soc.* **1958**, *41*, 390−397.
[11] T. Negas, R. S. Roth, H. S. Parker, D. B. Minor, *J. Solid State Chem.* **1974**, *9*, 297−307.
[12] H. M. O'Bryan Jr., J. Thomson, *J. Am. Ceram. Soc.* **1974**, *57*, 522−526.
[13] J. J. Ritter, R. S. Roth, J. E. Blendell, *J. Am. Ceram. Soc.* **1986**, *69*, 155−162.
[14] K. W. Kirby, B. A. Wechsler, *J. Am. Ceram. Soc.* **1991**, *74*, 1841−1847.
[15] R. S. Roth, J. H. Ritter, H. S. Parker, D. B. Minor, *J. Am. Ceram. Soc.* **1986**, *69*, 858−862.
[16] B. G. Gatehouse, G. Fallon, and R. S. Roth, unpublished results, **1986**.
[17] B. G. Gatehouse, private correspondence to R. S. Roth, Dec. 11, **1987**.
[18] R. D. Shannon, *J. Appl. Phys.* **1993**, *73*, 348−366.
[19] E. J. Gabe, Y. LePage, J.-P. Charland, F. L. Lee, P. S. White, *J. Appl. Crystallogr.* **1989**, *22*, 384−387.
[20] C. R. Hubbard, Y. Zhang, R. L. McKenzie, Certificate of Analysis, SRM 660, National Institute of Standards and Technology, Gaithersburg, MD, 20899 (**1989**).
[21] Program CELLSVD by C. K. Lowe-Ma, Naval Air Warfare Center Weapons Division Technical Publication 8128, September **1993**.
[22] R. G. Geyer, J. Mantese, J. Baker-Jarvis, *NIST Tech. Note 1371* (**1994**).
[23] N. E. Brese, M. O'Keeffe, *Acta Crystallogr., Sect. B* **1991**, *47*, 192−197; with updated $r_0$ parameters from http://www.ccp14.ac.uk/ccp/web-mirrors/i_d_brown/bond_valence_param/


Received December 17, 2003
Early View Article
Published Online May 5, 2004

  